Diverging biological roles among human monocyte subsets in the context of tuberculosis infection

Luciana Balboa[1*], Jorge Barrios-Payan[2¶] - Erika González-Domínguez[3¶], Claire Lastrucci[4,5], Geanncarlo Lugo-Villarino[4,5], Dulce Mata-Espinoza[2], Pablo Schierloh[1], Denise Kviatcovsky[1], Olivier Neyrolles[4,5], Isabelle Maridonneau-Parini[4,5], Carmen Sánchez-Torres[3], María del Carmen Sasiain[1&] - Rogelio Hernández-Pando[2&]

[1] Institute of Experimental Medicine-CONICET, National Academy of Medicine, Pacheco de Melo 3081 (1425), Buenos Aires, Argentina
[2] Department of Experimental Pathology, National Institute of Medical Sciences & Nutrition "Salvador Zubirán", Vasco de Quiroga 15, Sección 16, Delegación Tlalpan (14000), Mexico City, Mexico
[3] Department of Molecular Biomedicine, Center for Research and Advances Studies, National Polytechnic Institute, Av. Instituto Politécnico Nacional 2508, Gustavo A. Madero, San Pedro Zacatenco (07360), Mexico City, Mexico
[4] CNRS, Institut de Pharmacologie et de Biologie Structurale, 205 route de Narbonne (31077), Toulouse, France
[5] Institut de Pharmacologie et de Biologie Structurale, Université de Toulouse, Université Paul Sabatier, 118 route de Narbonne (31062), Toulouse, France

Key words: Bacterial Infection, Cell Movement, Monocytes, Mycobacterium Infections, Pulmonary, Tuberculosis.

Short title: Monocyte subsets in Tuberculosis

[*] Author for correspondence: Luciana Balboa
Address: Pacheco de Melo 3081 (1425), Buenos Aires, Argentina
E-mail: luciana_balboa@hotmail.com

[¶] These authors contributed equally to this work.
[&] These authors also contributed equally to this work.

Abstract
Circulating monocytes (Mo) play an essential role in the host immune response to chronic infections. We previously demonstrated that $CD16^{pos}$ Mo were expanded in Tuberculosis (TB) patients, correlated with disease severity and were refractory to dendritic cell differentiation. Here, we investigated whether human Mo subsets ($CD16^{neg}$ and $CD16^{pos}$) differed in their ability to influence the early inflammatory response against *Mycobacterium tuberculosis (Mtb)*. We first evaluated the capacity of the Mo subsets to migrate and engage a microbicidal response *in vitro*. Accordingly, $CD16^{neg}$ Mo were more prone to migrate in response to different mycobacteria-derived gradients, were more resistant to *Mtb* intracellular growth and produced higher reactive oxygen species than their $CD16^{pos}$ counterpart. To further assess the functional dichotomy among the human Mo subsets, we carried out an *in vivo* analysis by adapting a hybrid mouse model (SCID/Beige) to transfer each Mo subset, track their migratory fate during *Mtb* infection, and determine their impact on the host immune response. In *Mtb*-infected mice, the adoptively transferred $CD16^{neg}$ Mo displayed a higher lung migration index, induced a stronger pulmonary infiltration of murine leukocytes expressing pro- and anti-inflammatory cytokines, and significantly decreased the bacterial burden, in comparison to $CD16^{pos}$ Mo. Collectively, our results indicate that human Mo subsets display divergent biological roles in the context of *Mtb* infection, a scenario in which $CD16^{neg}$ Mo may contribute to the anti-mycobacterial immune response, while $CD16^{pos}$ Mo might promote microbial resilience, shedding light on a key aspect of the physiopathology of TB disease.

Introduction

Mycobacterium tuberculosis (Mtb) is the etiological agent of tuberculosis (TB) that remains one of the most devastating human diseases being responsible of ~1.5 million deaths worldwide each year. While TB mortality is slowing declining each year, it is still unacceptably high. In fact new, faster and better drugs are urgently needed to better control and deal with TB disease. The success of *Mtb* infection depends mainly on its ability to elude host immune responses, such as hampering the development of efficient antigen-presenting cells [1]. In this regard, as monocytes (Mo) can replenish tissue antigen-presenting cells (*i.e.* macrophages and dendritic cells), on demand [2], they represent an ideal target for immune evasion by *Mtb*.

Human blood Mo are conventionally subdivided into two major subsets based on CD16 expression: $CD14^{+}CD16^{-}$ ($CD16^{neg}$) and $CD14^{+}CD16^{+}$ ($CD16^{pos}$) [3]. We have previously demonstrated that human $CD16^{pos}$ Mo preferentially expand in TB patients, correlate with disease severity [4] and are refractory to dendritic cells differentiation [5]. Furthermore, while CCR5 and CCR2 are reported to be highly expressed on $CD16^{pos}$ and $CD16^{neg}$ Mo respectively in healthy donors [6, 35], we have found that these receptors are similarly expressed in both Mo subsets from patients with severe TB [4], suggesting a major alteration in the chemokine receptor repertoire as a consequence of disease. Together, these results suggest that different biological roles, including the migration capacity, among human Mo subsets might be modulated by the infection with *Mtb*.

Much of our knowledge on Mo migration and function during *Mtb* infection derives from the mouse model. Murine Mo subsets are distinguished as the "inflammatory" $Ly6C^{high}$ and the "patrolling" $Ly6C^{neg}$ cells. Through gene expression profiling, the $CD16^{neg}$ and $CD16^{pos}$ human Mo subsets have been correlated and compared to mouse $Ly6C^{high}$ and $Ly6C^{neg}$ Mo, respectively [6, 7]. Interestingly, $Ly6C^{high}$ Mo were found to be the major inducible nitric oxide synthase-producing cell population during pulmonary *Mtb* infection [8], and thus they may directly defend against mycobacterial infection. Also, increasing evidence implicates $Ly6C^{high}$ Mo in the activation and differentiation of CD4 T cell responses to mycobacterial infections [9, 10]. In spite of this, it was also shown that the CCL2-CCR2–dependent recruitment of Mo can be deleterious in part because they harbor live *Mtb* impairing microbial clearance [11]. Collectively, these reports have not only improved our understanding of murine Mo biology during mycobacterial infections, but also argue for the need to translate this knowledge into the human context. For this purpose, multiple strains of immunodeficient mice have been developed [12-14], such as SCID/Beige mice, which lack T and B lymphocytes, and have a defect on lysosomal biogenesis. Indeed, the SCID/Beige strain has been successfully used to investigate the role of human Mo subsets into the peritoneal cavity during inflammation [15].

In this study, we investigated whether human Mo subsets could contribute differently to the early immune response against *Mtb*. For this purpose, we employed two approaches: 1) an *in vitro* characterization of the capacity of the Mo subsets to migrate and engage a microbicidal response in the TB context; and 2) an *in vivo* analysis through the adaptation of a hybrid mouse model

(SCID/Beige) to transfer each human Mo subset, track their migratory fate during *Mtb* infection, and determine their impact on the host immune response.

Methods

Ethics statements

The research with human samples was carried out in accordance with the Declaration of Helsinki (2013) of the World Medical Association (further information in supplementary material).

Mice

C.B-17 SCID/Beige mice (Taconic Farms, Germantown, NY, USA) are homozygous for two genetic mutations which render them immunologically incompetent. They have a combined effect of *scid* (no T and B cells) and *beige* (defect in lysosomal trafficking regulator gene) mutations. Also, the *beige* mutation results in an impairment of natural killer (NK) cell activity [16]. Consequently these hybrid mice readily accept foreign cells.

Mtb growth

All procedures were performed in a laminar flow hood in a biosafety level III laboratory. *Mtb* H37Rv was grown in Middlebrook 7H9 broth (Difco, Detroit, MI, USA) supplemented with 10 % ADC (Difco), 0.05 % Tween-80, 0.5 % glycerol to mid-log phase before freezing at -80 ºC. Multiple vials were stored at -80 ºC until further use. Frozen *Mtb* stock were freshly thawed and reconstituted at room temperature at the time of infection. A vial of stock bacilli was diluted in saline to the final concentration of 2–4 × 10^5 colony forming unit (CFU) in 0.1 mL (for in vivo infections) or 1-10 × 10^4 CFU in 0.02 mL (for in vitro infections). Before infection, each stock vial was plated for CFU enumeration to reconfirm the standard concentration of the inoculum. The CFU concentration of stock vials was calculated by serial dilution and plating in multiple replicates on Middlebrook 7H11 agar (Difco) containing 0.5 % glycerol and 10 % oleic acid-albumin-dextrose-catalase (OADC) growth enrichment (Becton Dickinson, Cockysville, MD, USA). Plates were incubated for 21 days at 37 ºC prior to determination of CFU.

Human Mo subsets isolation

PBMCs were obtained by ficoll density gradient (Nycomed Pharma, New York, NY, USA) of buffy coats from healthy donors after signed informed consent. Human $CD16^{neg}$ and $CD16^{pos}$ Mo were purified by magnetic-activated cell sorting technology (Miltenyi Biotec, Auburn, CA, USA), as reported previously [15]. Staining with anti-CD14 and anti-CD16 mAbs showed >95 % $CD16^{neg}$ Mo in the $CD16^{neg}$ fraction and >85 % $CD16^{pos}$ Mo in the $CD16^{pos}$ fraction.

Transmembrane migration assay

Human Mo of each subset (4 x 10^5 cells in 75 µL) were placed in the upper chamber of a Transwell insert (5 µm pore size, 96-well plate; Corning Costar), and 230 µL of media (RPMI with 0.5 % FCS), or supernatants from *Mtb*-stimulated-pulmonary epithelial cells (A549) and –polymorphonuclear cells (PMN), or cell-free pleural effusions from TB patients, were placed in the lower chamber. After 3 hours, cells that had migrated to the lower chamber were removed and analyzed. The relative number of cells migrating was determined on a flow cytometer using Calibrite beads (BD Biosciences, San Jose, CA, USA), where a fixed number of beads was included in each sample and the

number of cells per 1,000 beads was evaluated. Data were normalized to the number of initial cells.

3D-migration assays

For 3D-migration assays, 100 µL of Matrigel (BD Bioscience) were polymerized in Transwell inserts as described previously [17]. The top of each matrix insert was seeded with 5 x 10^4 $CD16^{neg}$ or $CD16^{pos}$ Mo. The lower Transwell chamber was filled with both 250 µL of media (RPMI with 0.5 % FCS), and with 250 µL of either pleural fluid effusion from TB patients or supernatants from *Mtb*-infected pulmonary epithelial cells (A549), PMN or bone marrow derived-macrophages (BMDM). As control, we used 500 µL of media from non-infected cells. Cell migration was counted after 72 hrs, as described previously [17]. The percentage of cell migration was obtained as the ratio of cells within the matrix to the total number of counted cells.

Infection of SCID/Beige mice by *Mtb*

Briefly, 8-14 week-old SCID/Beige were anaesthetized in a gas chamber using sevofluorane at 0.1 mL/mouse, and each mouse was infected by orotracheal instillation with 2-4 × 10^5 live bacilli. In parallel, some mice were simultaneously transferred with human $CD16^{neg}$ and $CD16^{pos}$ Mo (1–5 x 10^6) by orotracheal instillation. Mice were maintained on the holder in a vertical position until normal breathing. Infected mice were maintained in groups of 3-5 in cages fitted with micro-isolators.

Determination of CFU from tissues

Cell suspensions from lungs and bronchial alveolar lavage (BAL) were thawed rapidly and four serial dilutions of each were done. Dilutions were spread onto duplicate plates containing Bacto Middlebrook 7H10 agar enriched with OADC. Plates were incubated for 21 days prior to determination of CFU.

Histopathological studies

For histology and automated morphometry analysis, left lungs were fixed by intratracheal perfusion with 4 % formaldehyde for 48 hours, sectioned through the hilum, and embedded in paraffin. Sections of 4 µm thickness were stained with haematoxylin and eosin. The percentages of infiltrating leukocytes were estimated using an automated image analyzer (Q Win Leica, Milton Keynes, United Kingdom).

Immunohistochemistry

Lung paraffin-embedded sections from *Mtb*-infected SCID/Beige mice were deparaffinized and rehydrated. Heat-induced antigen retrieval was achieved by incubating sections with sodium citrate 10 mM, pH 6.0 in a pressure cooker. The endogenous peroxidase activity was blocked 2 times incubating with 6 % H_2O_2 in methanol for 10 minutes. After blocking with Universal Blocking Buffer (Bio SB), tissue sections were incubated with primary antibodies for 1 hour at optimal dilutions previously determined. The following primary antibodies against tumor necrosis factor alpha (TNF) (rabbit polyclonal IgG;), IL-1β (goat polyclonal IgG), transforming growth factor beta (TGF-β) (rabbit polyclonal IgG) and IL-10 (goat polyclonal IgG) were used, all were purchased from Santa Cruz Biotechnology, CA, USA. Secondary biotinylated antibodies (biotin–anti-rabbit IgG or biotin–anti-goat IgG) were used to detect the binding of the primary

antibodies and, horseradish peroxidase (HRP)-conjugated avidin and 3,3-diaminobenzidine (DAB)–hydrogen peroxide were employed to develop the reaction. Tissue sections were counterstained with hematoxylin. For morphometry, 15 random fields from each section were studied. The percentage of positive cells for each cytokine was determined using an automated image analyzer (Q Win Leica).

Flow Cytometry

Cells were incubated with 20 µL of Fc-receptor blocking agent (Octagam, Octapharma Ltd, Coventry, UK) and incubated for 20 minutes. For the identification of human cells in mice tissue, cells were incubated with anti-human HLA-DR PE conjugated antibodies (clone G46-6, BD Biosciences) for 30 minutes at 4 ºC. This mAb does not cross-react with murine cells [15]. Data were acquired in a Guava Easy flow cytometer (Millipore, Bedford, MA, USA) and analyzed using the FCS Express Software (De Novo Software, Los Angeles, CA, USA). For the phenotypification of murine cells, cells were incubated with the following antibodies: anti-Ly6C (clone AL-21, APC-Cy7, BD Biosciences), anti-Ly6G (clone 1A8, PE, BD Biosciences), anti-CD11b (clone M1/70, eBioscience, San Diego, CA, USA); FITC), and anti-CD11c (clone CHL3, BD Pharmingen, San Jose, CA, USA; APC) for 30 minutes at 4 ºC. Data were acquired in a Cyan ADP flow cytometer.

Kinetics of intracellular replication of *Mtb* in human Mo

Human Mo of each subset were allow to adhere in 96 wells flat-plates and were cultured in RPMI with 10 % FCS for 24 hours (1 x 10^5 in 0.2 mL). Adherent cells were co-cultured in triplicate with bacilli at 1:1 ratio. After 2 hours of incubation, extracellular bacteria were removed gently by washing four times with pre-warmed PBS. After 2, 24, 48 or 96 hours infected MDM were subjected to complete lysis by mixing with 0.1 mL of 0.1 % SDS and incubated at room temperature for 10 minutes. Lysates were mixed thoroughly for ten times and neutralized by the addition of 0.1 mL of 20 % BSA in Middlebrook 7H9 broth. Thereafter lysates were serially diluted and plated, in triplicate, on 7H11 agar plates for CFU determination.

Oxidative Burst generation by *Mtb*-stimulated human Mo subsets

Intracellular Reactive Oxygen Species levels were measured by Dihydrorhodamine assays 123 (DHR, Sigma). DHR was dissolved in DMSO (20 µg/mL) and stored in aliquots at −70 °C until use. Briefly, 5 × 10^5 $CD16^{neg}$ and $CD16^{pos}$ were incubated with 0.1 mL DHR (5 µg/mL) for 15 minutes at 37 °C. Afterward, the gamma-irradiated *Mtb* H37Rv strain, kindly provided by J. Belisle (Colorado State University, Fort Collins, CO, USA), was added to the culture at 5*Mtb*:1Mo ratio for additional 20 minutes. After that, the fluorescent derivative, Rhodamine 123, was determined by FACS.

F-actin polymerization assay

$CD16^{neg}$ or $CD16^{pos}$ isolated Mo from healthy donors were adjusted to a concentration of 2 x 10^5 cell in 50 µL of PBS and they were let rest for 30 minutes at 37 ºC. Thereafter, cells were treated with 50 µL of cell-free PE or PBS for different times (0, 5, 15, 60 and 120 seconds). At the indicated time points, 50 µL of PFA 12 % was added for 10 min at room temperature. Cells

were washed and incubated for additional 20 minutes with a solution containing 4 x 10^{-7} M FITC-labeled phalloidin and triton X-100 0.1 % in PBS. The fixed cells were analyzed by flow cytometry within 1 hour after labeling. Alternatively, F-actin–stained Mo were attached to slides via Cytospin for their microscopic observation.

Statistical analysis

One-tailed paired or impaired t-test was applied on data sets with a normal distribution, whereas one-tailed Mann-Whitney (impaired test) or Wilcoxon (matched-paired test) tests were used otherwise (Prism software). $P<0.05$ was considered as the level of statistical significance.

Results

In vitro trafficking properties of human CD16^{neg} and CD16^{pos} Mo in response to mycobacteria-induced chemokine gradients

During pathogenic challenge, Mo exit the circulation and migrate towards the site of infection through different environments (*e.g.* intra-tissular) in response to chemo-attractant gradients. Taking into account the differential chemokine receptors repertoire displayed by Mo subsets [4, 18], we assessed the capacity of CD16^{neg} and CD16^{pos} Mo to migrate in two-dimensional (2D) and 3D environments in response to *Mtb*-induced chemo-attractant gradients. For these *in vitro* migration assays, isolated human Mo subsets were seeded onto the upper chamber of a transwell system either naked to assess 2D migration (Figure 1A) or filled with a Matrigel matrix (Figure 1B) extracted from tumors, with the lower compartment containing either cell-free pleural fluid effusion from TB patients, or conditioned media derived from *Mtb*-infected pulmonary epithelial cells (A549) or PMN leukocytes. Thereafter, migrating cells were quantified. As illustrated in Figure 1A, CD16^{neg} Mo migrated more efficiently than CD16^{pos} Mo in response to all chemo-attractant factors. Across Matrigel, the movement of cells requires proteolytic degradation of the extracellular matrix to create paths and is qualified as 'mesenchymal' [17]. As demonstrated in Figure 1B, CD16^{neg} Mo were more prone to migrate through Matrigel in response to mycobacteria-derived factors, compared to CD16^{pos} Mo. Since it is recognized that a rapid conversion of G-actin to F-actin is triggered in the initial phase of the chemotactic response [19], we then measured the effect of cell-free pleural fluid effusion from TB patients on actin polymerization in both Mo subsets. In line with their higher motility in different environments, CD16^{neg} Mo increased their F-actin content after exposure to tuberculous pleural fluid effusion in contrast to that observed for CD16^{pos} Mo (Figure 1C-D). Another important feature in the Mo recruitment into tissues is the interaction with endothelial and epithelial cells. Then we assessed their capacity to interact with alveolar epithelial cells, and we observed no differences among the Mo subsets in their ability to adhere to A549 cells (Figure S1). Therefore, despite showing a comparable ability to interact with lung epithelial cells, both Mo subsets differ in their migratory behavior being the CD16^{neg} subset capable to readily respond to mycobacteria-induced chemokine gradients unlike the CD16^{pos} subset.

Microbicidal activities displayed by Mo subsets

Since the antimicrobial activity of human Mo is crucial for the eradication of intracellular pathogens, we investigated whether Mo subsets differ in their ability to control *Mtb* intracellular growth. We found lesser number of bacteria growing in CD16^{neg} Mo in comparison to their CD16^{pos} counterpart at different times post-infection when considering the CFU recovered from the whole Mo lysates (Figure 1E). To take into account that *Mtb*-infected CD16^{pos} Mo display a higher mortality rate compared to CD16^{neg} Mo [20], we also measure bacterial growth per cell. Accordingly, we confirmed that the CD16^{pos} were more permissive to Mtb replication than CD16^{neg} (Figure 1F). Based on these results, we then examined the oxidative microbicidal activity of Mo subsets in response to irradiated *Mtb*; the killed version was used in order to avoid the well described suppressive effects mediated by live *Mtb* [21]. To this end, the conversion of Dihydrorhodamine 123 (DHR) into its fluorescent form triggered by reactive oxygen species such as peroxide and peroxynitrite was analyzed in CD16^{neg}

and CD16^{pos} Mo after a 20-minute challenge with irradiated *Mtb*. In line with the results from CFU assays, CD16^{neg} Mo induced higher production of oxygen reactive species after *Mtb* exposure (Figure 1G). Altogether, these results indicate that human Mo subsets differ drastically in the ability to eliminate *Mtb*.

Potential of CD16^{neg} and CD16^{pos} Mo to traffic from the alveolar spaces to lung parenchyma in an in vivo environment

In order to assess the migration patterns of human Mo subsets *in vivo*, we transferred human CD16^{neg} or CD16^{pos} Mo orotracheally into *Mtb*-infected SCID/Beige mice, and compared their abilities to traffic from the alveolar spaces to the lung parenchyma (see supplementary information for further details on the human Mo engraftment). After 24 h, human cells from BAL and lungs were quantified as the ratio between the numbers of recovered HLA-DR^{pos} cells and total inoculated cells. Under infectious conditions, the percentages of HLA-DR^{pos} cells recovered from CD16^{neg} Mo-transferred mice were higher in lungs (Figure 2A-B) and lower in BAL (Figure 2C-D), which is consistent with the induction of cell recruitment from the alveolar space to the lung parenchyma in response to the infection. Unlike CD16^{neg} Mo, the recovery of HLA-DR^{pos} cells in lungs and BAL from CD16^{pos} Mo-transferred mice did not differ between steady state and infectious conditions (Figure 2B and D). In fact, the percentages of CD16^{pos} Mo recovered under steady state conditions were higher in lungs and lower in BAL compared to CD16^{neg} Mo (Figure 2A and C). Considering that CD16^{pos} circulating Mo are prone to undergo cell death [20], we tested whether this process could be involved during the engraftment of human Mo under infectious conditions. However, no differences between the percentages of 7-AAD^{pos}/HLA-DR^{pos} cells recovered from lungs of CD16^{neg} and CD16^{pos} Mo-transferred SCID/Beige mice were found (Figure 2E). Altogether these results suggest that unlike human CD16^{pos} Mo, the CD16^{neg} subset is specifically predisposed to respond to *Mtb* infection by increasing their mobility towards the infected site.

As we transferred human cells into a xenogeneic host, we wondered whether the putative murine ortholog Mo subsets follow the same migration pattern as their human counterparts upon *Mtb* infection. To this end, we evaluated the dynamics of the murine Ly6C^{high} Mo subset in different tissues from *Mtb*-infected BALB/c mice. As depicted in Figure S5, the percentage of Ly6C^{high} Mo increased in lungs and BAL at early stages of the infection correlating with its decrease in blood, suggesting that this subset migrates very early from blood to the infected site. Based on the proposed homology of Mo subsets between species, this result may be in line with our in vitro assays described above.

Effect of human CD16^{neg} or CD16^{pos} Mo on the outcome of *Mtb*-infected SCID/Beige mice

Having found a differential migration pattern to the site of infection between human Mo subsets, we wondered whether the presence of CD16^{neg} or CD16^{pos} Mo during the early stage of the inflammatory response would affect the outcome of the infection against *Mtb*. We first determined the production of cytokines by IHC in lung tissue sections from CD16^{neg} or CD16^{pos} Mo-transferred mice infected (or not), as compared to mice that were also infected (or not) but lack human Mo. *Mtb* infected mice showed numerous large

macrophages with abundant cytoplasm and peripheral nucleus corresponding to activated cells (Figure 3, right panels). These cells were located in the alveolar capillary interstitium and alveolar spaces, being more abundant in $CD16^{neg}$ Mo-transferred mice. We found higher levels of the anti-inflammatory cytokines IL-10 and TGF-β in the lung of $CD16^{neg}$ Mo-transferred mice compared to $CD16^{pos}$ Mo-transferred (Figure 3A-B), whereas both Mo subsets induce high levels of TNF and IL-1β (Figure 3C-D). Interestingly, uninfected $CD16^{pos}$ Mo-transferred mice showed a high basal IL-1β production.

Another feature of the early inflammatory response is the recruitment of leukocytes to the site of infection. This was evaluated by measuring the infiltration area of murine leukocytes after hematoxylin and eosin staining of lung tissue sections. Under steady conditions, $CD16^{pos}$ Mo induced higher recruitment of leukocytes; under infectious conditions, however, the $CD16^{neg}$ Mo induced higher recruitment of leukocytes (Figure 4A-B). Therefore, while the transfer of $CD16^{pos}$ Mo was enough to induce the recruitment of IL-$1\beta^{pos}$ leukocytes in lungs, $CD16^{neg}$ Mo transfer promotes leukocytes attraction and cytokines production upon infection with *Mtb*.

Finally, the bacterial load associated to airways tissue (lungs and BAL) in $CD16^{neg}$ and $CD16^{pos}$ Mo-transferred infected mice was compared. As shown in Figure 4C, a significant decrease in the bacterial load was observed in the lungs from mice with adoptive transfer of $CD16^{neg}$ Mo compared to non-transferred or $CD16^{pos}$ Mo transferred-mice. Reciprocally, higher bacillary loads were detected in BAL from mice with adoptive transfer of $CD16^{pos}$ Mo (Figure 4D).

Discussion

Inflammatory cell recruitment is essential for antituberculous host immune defense. In particular, Mo are highly sensitive and reactive to pathogen-derived molecules, and can quickly respond to microbial-stimuli to inhibit pathogens at early stages of infection. In this work, we have shown through different experimental approaches that human Mo subsets have different migration pattern to lungs in response to *Mtb* infection. In particular, we found that $CD16^{neg}$ human Mo were more prone to migrate in response to mycobacteria-derived gradients. These results are further supported by the restricted actin fibers polymerization induction found in $CD16^{neg}$ Mo upon stimulation with tuberculous pleural effusions, which is central for regulating cellular motility [22]. Despite this, human Mo subsets show a comparable ability to cross the endothelium [23] and to attach to the alveolar epithelium as herein shown. Therefore, $CD16^{neg}$ Mo may have enhanced responsiveness to *Mtb*-induced chemoattractants in comparison to $CD16^{pos}$ Mo. Differences in the concentration of molecular components such as adhesion receptors, cytoskeletal-linking proteins, and extracellular matrix ligands, may explain the qualitative differences in migratory behavior between Mo subsets [24]. Hence, we propose that at early events after *Mtb* infection, $CD16^{pos}$ Mo may display lesser expression of chemokines receptors that promote the infiltration to lungs compared to $CD16^{neg}$ as stated by others [25]. Yet, it is possible that this unresponsiveness to *Mtb*-induced chemoattractants displayed by $CD16^{pos}$ Mo may be overcame as the infection progresses, which would be in agreement with our previous finding that $CD16^{pos}$ Mo acquired CCR2 expression in TB patients with severe disease [4].

The immune system in both human and murine contexts is highly conserved and functions in a similar fashion. Nevertheless, when a particular immune cell subtypes is compared between the two species, they may display distinct characteristics. Considering that the individual biologic functions of human Mo subsets *in vivo* are not completely understood [7], we decided to use the SCID/Beige mice hybrids for modeling the effect of human Mo transference on the outcome of *Mtb* infection. In fact, we could study the migration of human Mo in response to *Mtb* infection. This is in agreement with other experimental approaches on humanized mice models in which human bone marrow precursors could differentiate into tissue macrophages, including pulmonary macrophages, under physiological and inflammatory conditions [26, 27]. In our hands, this SCID/Beige mice model allows for rapid analysis of human immune cell behavior because the transferred cells are short-lived and functionally mature. Considering the poor recovery of human derived-cells obtained when transferring the Mo by intravenous route into SCID/Beige mice, we inoculated them orotracheally and examined the migration route from the alveolar space to the lung interstitium. In fact, it has been reported that macrophages transmigrate back to the basal side of the epithelium after phagocytosis in order to participate to the presentation of antigens [28], thus transmigration back to the basal side of the epithelium is an important behavior of macrophages [29]. In our SCID/Beige model, $CD16^{neg}$ Mo were able to migrate to the infected site more efficiently than $CD16^{pos}$ Mo, supporting the differential migration patterns observed in vitro.

A limitation of our model is the absence of adaptive immune response in these immunocompromised mice. In this regard, our results require careful consideration given that the effector function of Mo in a normal inflammatory milieu may be significantly different to what we observed in this study. Also, this limitation impedes an examination of the effect of each human Mo subset on the initiation of the acquired immune response. Interestingly, it has been demonstrated that infected inflammatory Mo-derived dendritic cells are essential for the transport of *Mtb* to the local lymph node that, although being relatively inefficient at activating CD4 T cells, they can release *Mtb* antigens for uptake and presentation by uninfected resident lymph node dendritic cells [10, 30]. These results support the hypothesis that different Mo subsets are committed for specific functions not only at early stages of the infection, as herein demonstrated, but also when the priming of antigen-specific CD4 T cells may take place. In this study, we observed a high influx of Ly6C^{high} Mo into lungs and BAL in parallel with a marked decrease in blood at the 14th day pi (Figure S4C-D), when the adaptive immune response is supposed to be initiated [31]. This result suggests that the arrival of this subset at the infected site could be important to modulate the acquired immune response, supporting the already demonstrated essential role for CCR2^{+} inflammatory Mo during *Mtb*-specific T cell priming [30]. Moreover, it has recently been shown that Ly6C^{low} Mo are precursors of pulmonary resident macrophages [32], which could be in agreement with our results assuming the equivalence between the murine Ly6C^{low} and the human CD16^{pos} Mo subsets. Although we do not provide direct evidence for this homology, our results support previous reports that postulate Ly6C^{high} as the homologue for CD16^{neg} Mo [7].

In general, tissue macrophages of differing ontological origins coexist, but whether resident and newly recruited macrophages possess similar functions during inflammation is unclear. The lung macrophage populations have been described as alveolar macrophages, which originate of embryonic hematopoietic stem cells-derived, and CD11b^{pos} macrophages of unknown origin [33]. It is well established that inflammation triggers blood Mo recruitment and differentiation into macrophages [2, 33]. Therefore, circulating Mo may replenish lung macrophages during TB. Intriguingly, our results suggest that the nature of Mo subset together with environmental cues can dictate the macrophage functions.

We have observed an increased migration ability of CD16^{pos} human Mo under steady state conditions in our *in vivo* model, which may be in agreement with their higher expression of genes connected to migration and transendothelial motility (LSP1, LYN, CFL1, MYL6), according to the transcriptome analysis in purified Mo subsets from human blood [34]. Despite this, it is important to take into consideration that the inoculation itself might alter steady dynamics (*i.e.*, injured tissue recruits Mo), making it difficult to draw conclusions on the behavior of Mo subsets under steady state conditions.

Additionally, we showed that human Mo subsets can impact differently on the host immune response against *Mtb*. The recruitment of leukocytes into the alveolar spaces and, even more, the establishment of a balance pro- and anti-inflammatory cytokines production, are crucial for clearing infections and

resolving the inflammatory response. In this regard, we demonstrated that Mo subsets display different abilities to orchestrate cytokines production by pulmonary cells and leukocyte recruitment. While $CD16^{neg}$ Mo induce a balanced production of cytokines together with leukocyte recruitment under infectious conditions, $CD16^{pos}$ Mo induce IL-1β production and leukocyte recruitment under non infectious conditions. The virulence of pathogens depends on their ability to fine-tune the inflammatory responses to a pitch that is optimal for *Mtb* growth [35]. Increased disease severity in humans can also occur for fundamentally opposite reasons: an inadequate host immune response to infection or an excessive one [36]. Therefore, the balance of inflammation is critical for determining the outcome of infection at a systemic level. Virulent mycobacteria themselves have evolved to disrupt the fine balance of pro- and anti-inflammatory cues required for host protection [37]. In this sense, we speculate that the regulated inflammatory response triggered by $CD16^{neg}$ Mo may prolong host survival by preventing immunopathology. Besides, both human Mo subsets display different abilities to control mycobacterial replication given that human $CD16^{pos}$ Mo are more permissive for *Mtb* growth and induce lower levels of respiratory burst after *Mtb* exposure. According to our previous results, the severity of TB in humans is associated to the progressive accumulation of $CD16^{pos}$ Mo in the blood [4], leading to the predominance of a more permissive host cell and possibly contributing to the dissemination of *Mtb*. As we used Mo subsets isolated from healthy individuals, we consider that our results may explain the migration behaviors that take place during the early events of the infection, given that at advanced stages of the infection the chemokine receptors profile is altered in Mo from TB patients [4]. Therefore, it is possible that these more permissive $CD16^{pos}$ Mo may acquire an improved migration ability towards the infected site once the mycobacteria can govern the host-pathogen interaction and promote the disease. This hypothesis needs to be tested. While our study may be of clinical importance that still requires further validation to compensate for the limitations imposed by our hybrid *in vivo* model, we propose a model for the dynamics of the influx of Mo subsets according to the stage of *Mtb* infection and how it may impact on the ongoing immune response (Figure S6).

Our results highlight two main aspects that should be taken into account when evaluating the different roles of Mo subsets in infectious diseases, 1) the existence of intrinsic functional plasticity between $CD16^{pos}$ and $CD16^{neg}$ Mo, including their inherent commitments and; 2) the extrinsic functional plasticity driven by the specific microenvironment, which explains why a given subset can display different biological functions under steady state or infectious conditions including immune evasion mechanisms triggered by the pathogen.

Collectively, these results provide clear evidence for a differential contribution of human Mo subsets throughout the course of the infection, shedding light on a key aspect of the physiopathology of TB. While $CD16^{neg}$ Mo may contribute to the anti-mycobacterial immune response, $CD16^{pos}$ Mo might promote microbial resilience.

Clinical Perspectives

- In 2013, TB was considered the second leading cause of death from a single infectious agent (*global TB report, WHO, 2014*). While TB mortality is slowing declining each year, it is still unacceptably high and without new and improved TB treatment regimens, including treatment for those suffering from drug-resistant TB and co-infected with HIV/AIDS, the reduction and eventual eradication of the disease cannot be achieved.
- Here we demonstrate that human monocyte subsets play different roles in promoting or hampering the host immune responses to infection with *Mtb*.
- The further understanding of how monocytes subsets arrive to the infected site and what they do once there, can shed light on a key aspect of the physiopathology of TB and may help to inform future vaccine and drug development strategies.

Author contribution

LB, CST, MCS and RHP conceived and designed the experiments. LB, JBP, EGD, CL, GLV, DME, PS and DK performed the experiments. LB, CL, GLV, PS and DK analyzed the data. ON, IMP, CST, MCS and RHP contributed reagents/materials/analysis tools. LB, CL, GLV, ON, IMP, CST, MCS and RHP contributed to the writing of the manuscript. All authors read and approved the final manuscript.

Acknowledgments

We thank Juan Carlos León-Contreras, Pablo Vallecorsa and Dr. Roberto Meiss for excellent technical support. We also thank the staff of the Hemotherapy Service of the Garrahan Hospital (Buenos Aires), the Etablissement Français du Sang (Toulouse) and the Hospital C.M.N. La Raza (IMSS, Mexico City) for the contribution with donor's recruitment. This study was supported by the National Agency for Science and Technology Promotion, Ministry of Science of Argentina (PICT 2011-0572 by MCS and PICT 2012-0221 by LB), by the Mexican National Council of Science and Technology (SEP-CONACYT n° 179388 by CST and CONACyT n° 84456 by RHP), by the French National Research Agency (ANR 2010-01301 and MigreFlame by IMP an ANR-12-BSV3-0002 ANR-funded grant B-TB by ON), and by the Fondation pour la Recherche Médicale (FRM, DEQ 20110421312 by IMP). EGD was the recipient of a CONACYT pre-doctoral scholarship (no. 302832) and LB was awarded a fellowship by the Ministry of Foreign Affairs of Mexico. The funders had no role in study design, data collection and analysis, decision to publish, or preparation of the manuscript.

Funding

This work was supported by grants from the National Agency for Science and Technology Promotion, Ministry of Science of Argentina, contracts: PICT 2011-0572 (MCS) and PICT 2012-0221 (LB); from the Mexican National Council of Science and Technology, contracts: 179388 (CST) and 84456 (RHP); from the French National Research Agency, contracts: ANR 2010-01301 MigreFlame (MP) and ANR-12-BSV3-0002 ANR-funded grant B-TB (ON), and from the Fondation pour la Recherche Médicale, contract: FRM, DEQ 20110421312 (IMP). EGD is the recipient of a Mexican National Council of Science and

Technology pre-doctoral scholarship (302832). LB was awarded a fellowship by the Ministry of Foreign Affairs of Mexico. The funders had no role in study design, data collection and analysis, decision to publish, or preparation of the manuscript.

References

1 Balboa, L., Romero, M. M., Yokobori, N., Schierloh, P., Geffner, L., Basile, J. I., Musella, R. M., Abbate, E., de la Barrera, S., Sasiain, M. C. and Aleman, M. (2010) Mycobacterium tuberculosis impairs dendritic cell response by altering CD1b, DC-SIGN and MR profile. Immunol Cell Biol. **88**, 716-726

2 Ginhoux, F. and Jung, S. (2014) Monocytes and macrophages: developmental pathways and tissue homeostasis. Nat Rev Immunol. **14**, 392-404

3 Ziegler-Heitbrock, L. (2007) The CD14+ CD16+ blood monocytes: their role in infection and inflammation. J Leukoc Biol. **81**, 584-592

4 Balboa, L., Romero, M. M., Basile, J. I., Sabio y Garcia, C. A., Schierloh, P., Yokobori, N., Geffner, L., Musella, R. M., Castagnino, J., Abbate, E., de la Barrera, S., Sasiain, M. C. and Aleman, M. (2011) Paradoxical role of CD16+CCR2+CCR5+ monocytes in tuberculosis: efficient APC in pleural effusion but also mark disease severity in blood. J Leukoc Biol. **90**, 69-75

5 Balboa, L., Romero, M. M., Laborde, E., Sabio, Y. G. C. A., Basile, J. I., Schierloh, P., Yokobori, N., Musella, R. M., Castagnino, J., de la Barrera, S., Sasiain, M. C. and Aleman, M. (2013) Impaired dendritic cell differentiation of CD16-positive monocytes in tuberculosis: role of p38 MAPK. Eur J Immunol. **43**, 335-347

6 Cros, J., Cagnard, N., Woollard, K., Patey, N., Zhang, S. Y., Senechal, B., Puel, A., Biswas, S. K., Moshous, D., Picard, C., Jais, J. P., D'Cruz, D., Casanova, J. L., Trouillet, C. and Geissmann, F. (2010) Human CD14dim monocytes patrol and sense nucleic acids and viruses via TLR7 and TLR8 receptors. Immunity. **33**, 375-386

7 Ingersoll, M. A., Spanbroek, R., Lottaz, C., Gautier, E. L., Frankenberger, M., Hoffmann, R., Lang, R., Haniffa, M., Collin, M., Tacke, F., Habenicht, A. J., Ziegler-Heitbrock, L. and Randolph, G. J. (2010) Comparison of gene expression profiles between human and mouse monocyte subsets. Blood. **115**, e10-19

8 Shi, C. and Pamer, E. G. (2011) Monocyte recruitment during infection and inflammation. Nat Rev Immunol. **11**, 762-774

9 Peters, W., Scott, H. M., Chambers, H. F., Flynn, J. L., Charo, I. F. and Ernst, J. D. (2001) Chemokine receptor 2 serves an early and essential role in resistance to Mycobacterium tuberculosis. Proc Natl Acad Sci U S A. **98**, 7958-7963

10 Srivastava, S. and Ernst, J. D. (2014) Cell-to-cell transfer of M. tuberculosis antigens optimizes CD4 T cell priming. Cell Host Microbe. **15**, 741-752

11 Antonelli, L. R., Gigliotti Rothfuchs, A., Goncalves, R., Roffe, E., Cheever, A. W., Bafica, A., Salazar, A. M., Feng, C. G. and Sher, A. (2010) Intranasal Poly-IC treatment exacerbates tuberculosis in mice through the pulmonary recruitment of a pathogen-permissive monocyte/macrophage population. J Clin Invest. **120**, 1674-1682

12 Shultz, L. D., Brehm, M. A., Garcia-Martinez, J. V. and Greiner, D. L. (2012) Humanized mice for immune system investigation: progress, promise and challenges. Nat Rev Immunol. **12**, 786-798
13 Brehm, M. A. and Shultz, L. D. (2012) Human allograft rejection in humanized mice: a historical perspective. Cell Mol Immunol. **9**, 225-231
14 Meyerrose, T. E., Herrbrich, P., Hess, D. A. and Nolta, J. A. (2003) Immune-deficient mouse models for analysis of human stem cells. Biotechniques. **35**, 1262-1272
15 Aguilar-Ruiz, S. R., Torres-Aguilar, H., Gonzalez-Dominguez, E., Narvaez, J., Gonzalez-Perez, G., Vargas-Ayala, G., Meraz-Rios, M. A., Garcia-Zepeda, E. A. and Sanchez-Torres, C. (2011) Human CD16+ and CD16- monocyte subsets display unique effector properties in inflammatory conditions in vivo. J Leukoc Biol. **90**, 1119-1131
16 Mosier, D. E., Stell, K. L., Gulizia, R. J., Torbett, B. E. and Gilmore, G. L. (1993) Homozygous scid/scid;beige/beige mice have low levels of spontaneous or neonatal T cell-induced B cell generation. J Exp Med. **177**, 191-194
17 Van Goethem, E., Poincloux, R., Gauffre, F., Maridonneau-Parini, I. and Le Cabec, V. (2010) Matrix architecture dictates three-dimensional migration modes of human macrophages: differential involvement of proteases and podosome-like structures. J Immunol. **184**, 1049-1061
18 Weber, C., Belge, K. U., von Hundelshausen, P., Draude, G., Steppich, B., Mack, M., Frankenberger, M., Weber, K. S. and Ziegler-Heitbrock, H. W. (2000) Differential chemokine receptor expression and function in human monocyte subpopulations. J Leukoc Biol. **67**, 699-704
19 Wallace, P. J., Wersto, R. P., Packman, C. H. and Lichtman, M. A. (1984) Chemotactic peptide-induced changes in neutrophil actin conformation. J Cell Biol. **99**, 1060-1065
20 Castano, D., Barrera, L. F. and Rojas, M. (2011) Mycobacterium tuberculosis alters the differentiation of monocytes into macrophages in vitro. Cell Immunol. **268**, 60-67
21 Lugo-Villarino, G., Verollet, C., Maridonneau-Parini, I. and Neyrolles, O. (2011) Macrophage polarization: convergence point targeted by mycobacterium tuberculosis and HIV. Front Immunol. **2**, 43
22 Pollard, T. D. and Borisy, G. G. (2003) Cellular motility driven by assembly and disassembly of actin filaments. Cell. **112**, 453-465
23 Randolph, G. J., Sanchez-Schmitz, G., Liebman, R. M. and Schakel, K. (2002) The CD16(+) (FcgammaRIII(+)) subset of human monocytes preferentially becomes migratory dendritic cells in a model tissue setting. J Exp Med. **196**, 517-527
24 Lauffenburger, D. A. and Horwitz, A. F. (1996) Cell migration: a physically integrated molecular process. Cell. **84**, 359-369
25 Geissmann, F., Jung, S. and Littman, D. R. (2003) Blood monocytes consist of two principal subsets with distinct migratory properties. Immunity. **19**, 71-82
26 Rathinam, C., Poueymirou, W. T., Rojas, J., Murphy, A. J., Valenzuela, D. M., Yancopoulos, G. D., Rongvaux, A., Eynon, E. E., Manz, M. G. and Flavell, R. A. (2011) Efficient differentiation and function of human macrophages in humanized CSF-1 mice. Blood. **118**, 3119-3128
27 Li, Y., Chen, Q., Zheng, D., Yin, L., Chionh, Y. H., Wong, L. H., Tan, S. Q., Tan, T. C., Chan, J. K., Alonso, S., Dedon, P. C., Lim, B. and Chen, J.

(2013) Induction of functional human macrophages from bone marrow promonocytes by M-CSF in humanized mice. J Immunol. **191**, 3192-3199
28 Guidi-Rontani, C. (2002) The alveolar macrophage: the Trojan horse of Bacillus anthracis. Trends Microbiol. **10**, 405-409
29 Ding, P., Wu, H., Fang, L., Wu, M. and Liu, R. (2014) Transmigration and phagocytosis of macrophages in an airway infection model using four-dimensional techniques. Am J Respir Cell Mol Biol. **51**, 1-10
30 Samstein, M., Schreiber, H. A., Leiner, I. M., Susac, B., Glickman, M. S. and Pamer, E. G. (2013) Essential yet limited role for CCR2+ inflammatory monocytes during Mycobacterium tuberculosis-specific T cell priming. Elife. **2**, e01086
31 Wolf, A. J., Linas, B., Trevejo-Nunez, G. J., Kincaid, E., Tamura, T., Takatsu, K. and Ernst, J. D. (2007) Mycobacterium tuberculosis infects dendritic cells with high frequency and impairs their function in vivo. J Immunol. **179**, 2509-2519
32 Yona, S., Kim, K. W., Wolf, Y., Mildner, A., Varol, D., Breker, M., Strauss-Ayali, D., Viukov, S., Guilliams, M., Misharin, A., Hume, D. A., Perlman, H., Malissen, B., Zelzer, E. and Jung, S. (2013) Fate mapping reveals origins and dynamics of monocytes and tissue macrophages under homeostasis. Immunity. **38**, 79-91
33 Epelman, S., Lavine, K. J. and Randolph, G. J. (2014) Origin and Functions of Tissue Macrophages. Immunity. **41**, 21-35
34 Zawada, A. M., Rogacev, K. S., Rotter, B., Winter, P., Marell, R. R., Fliser, D. and Heine, G. H. (2011) SuperSAGE evidence for CD14++CD16+ monocytes as a third monocyte subset. Blood. **118**, e50-61
35 Stanley, S. A. and Cox, J. S. (2013) Host-pathogen interactions during Mycobacterium tuberculosis infections. Curr Top Microbiol Immunol. **374**, 211-241
36 Tobin, D. M., Roca, F. J., Oh, S. F., McFarland, R., Vickery, T. W., Ray, J. P., Ko, D. C., Zou, Y., Bang, N. D., Chau, T. T., Vary, J. C., Hawn, T. R., Dunstan, S. J., Farrar, J. J., Thwaites, G. E., King, M. C., Serhan, C. N. and Ramakrishnan, L. (2012) Host genotype-specific therapies can optimize the inflammatory response to mycobacterial infections. Cell. **148**, 434-446
37 Volkman, H. E., Pozos, T. C., Zheng, J., Davis, J. M., Rawls, J. F. and Ramakrishnan, L. (2010) Tuberculous granuloma induction via interaction of a bacterial secreted protein with host epithelium. Science. **327**, 466-469

Figure 1

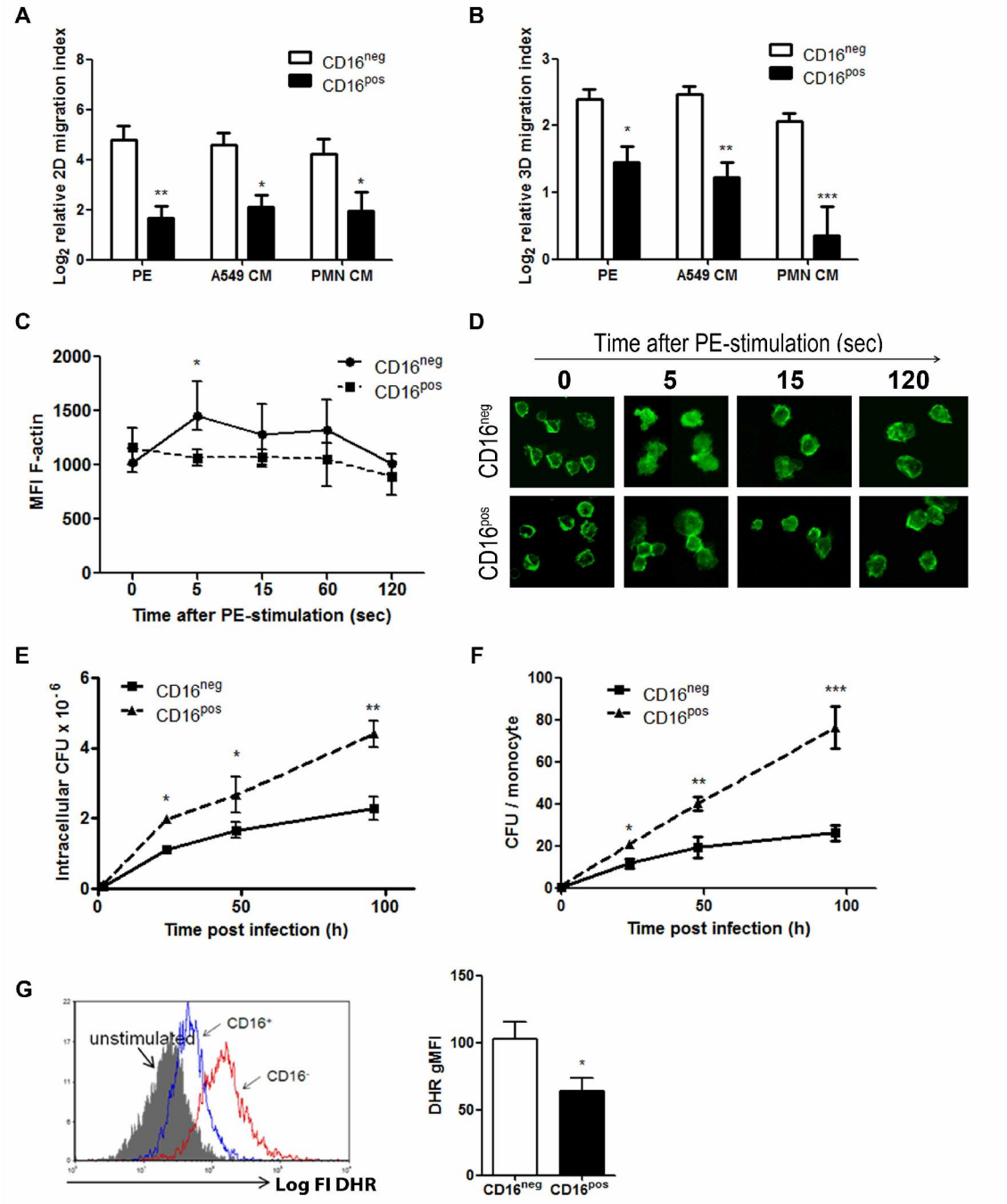

Figure 1. Migration and microbicidal properties of CD16^{neg} and CD16^{pos} Mo in response to *Mtb*. Isolated human Mo subsets were seeded onto the upper chamber of a transwell system (A) or on the Matrigel surface (B) in response to either control medium (-), cell-free pleural effusions from TB patients (PE), conditioned medium from *Mtb*-stimulated-pulmonary epithelial cells (A549-CM) or -PMN (PMN-CM). The relative migration index, defined as the numbers of migrating cells under an inflammatory condition relative to the control medium, is shown for each experimental condition. Data are presented as log2 ratios, and represent the average of 5 independent donors of monocytes. Statistical analysis: *, $p < 0.05$; ***, $p < 0.001$. (C) Time course analysis of actin polymerization in human Mo subsets after PE exposure expressed as specific mean fluorescence intensity (MFI) Data are the average of four independent

experiments. Statistical analysis: *P<0.05, $CD16^{neg}$ Mo vs $CD16^{pos}$ Mo. (D) Representative images of F-actin–stained in PE-treated Mo subsets for the indicated periods. (E-F) Kinetics of the intracellular CFU obtained from $CD16^{neg}$ or $CD16^{pos}$ Mo infected with *Mtb*, expressed as absolute CFU numbers (E) and CFU numbers relative to viable Mo numbers (F). Results are the mean ± SEM of three independent experiments, each carried out in triplicate. *P< 0.05. (G) Levels of respiratory burst estimated by dihydrorhodamine (DHR) fluorescence of unstimulated and *Mtb*-stimulated $CD16^{neg}$ and $CD16^{pos}$ Mo. A representative histogram is shown. Results are the geometric mean fluorescence intensity values ± SEM of eight independent experiments. *P< 0.05.

Figure 2

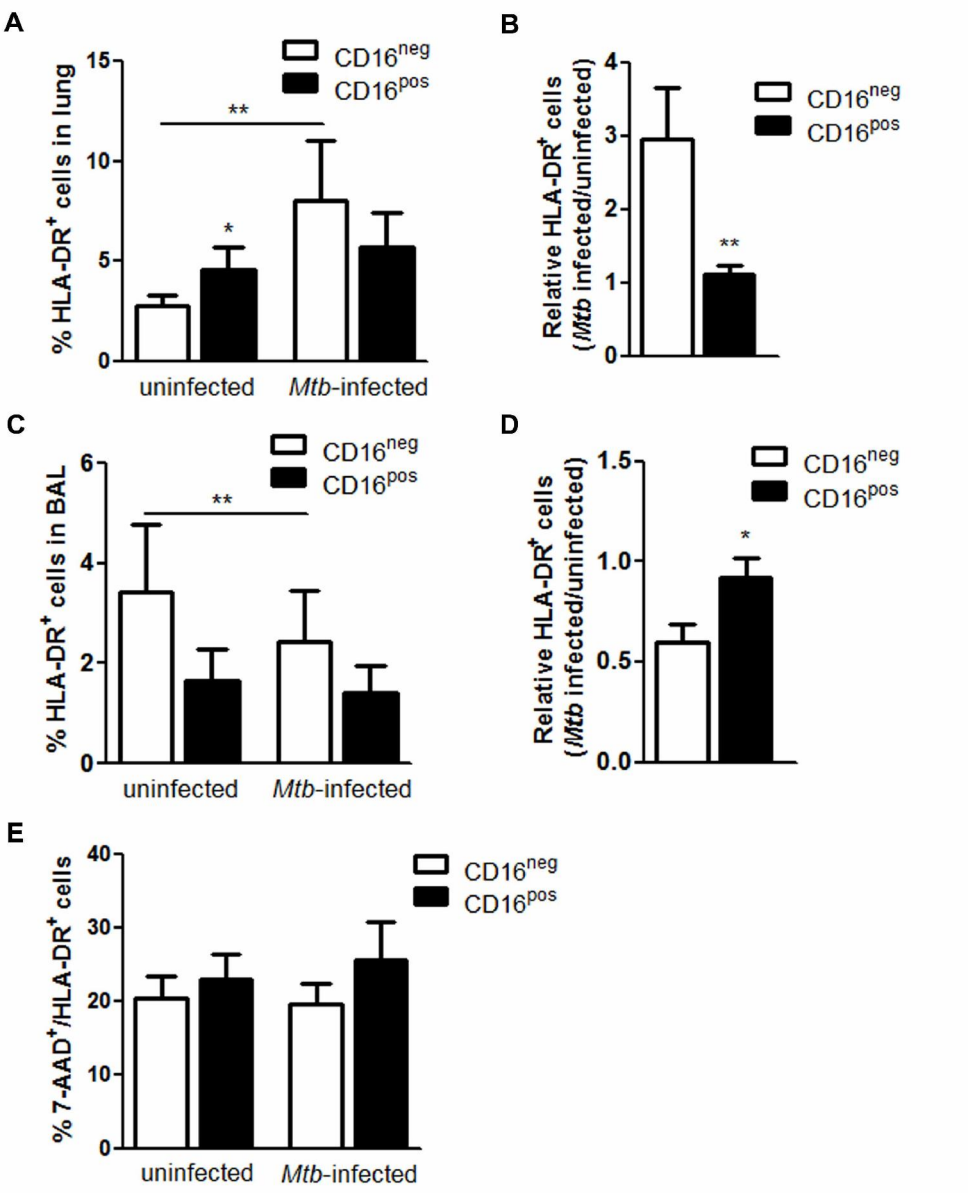

Figure 2. Migration patterns of human Mo subsets in an in vivo environment. Percentages of HLA-DR^{pos} human cells derived from CD16^{neg} or CD16^{pos} Mo recovered from lungs (A) and BAL (C) in uninfected or *Mtb*-infected SCID/Beige mice determined by flow cytometry. Percentages were calculated as numbers of recovered HLA-DR^{pos} cells and total inoculated human cells. Relative recovery of human cells derived from CD16^{neg} or CD16^{pos} Mo of lungs (B) and BAL (D) were estimated as the numbers of recovered HLA-DR^{pos} cells from *Mtb*-infected mice relative to uninfected mice. Data are the average of ten independent experiments. Statistical analysis: *P<0.05, **P<0.01, CD16^{neg} Mo vs CD16^{pos} Mo, or comparisons are indicated by lines. (E) Percentages of death cells (7-AAD^{pos}) among HLA-DR^{pos} human cells derived from CD16^{neg} or CD16^{pos} Mo recovered from lungs in uninfected or *Mtb*-infected SCID/Beige mice determined by flow cytometry. Data are the average of five independent experiments.

Figure 3

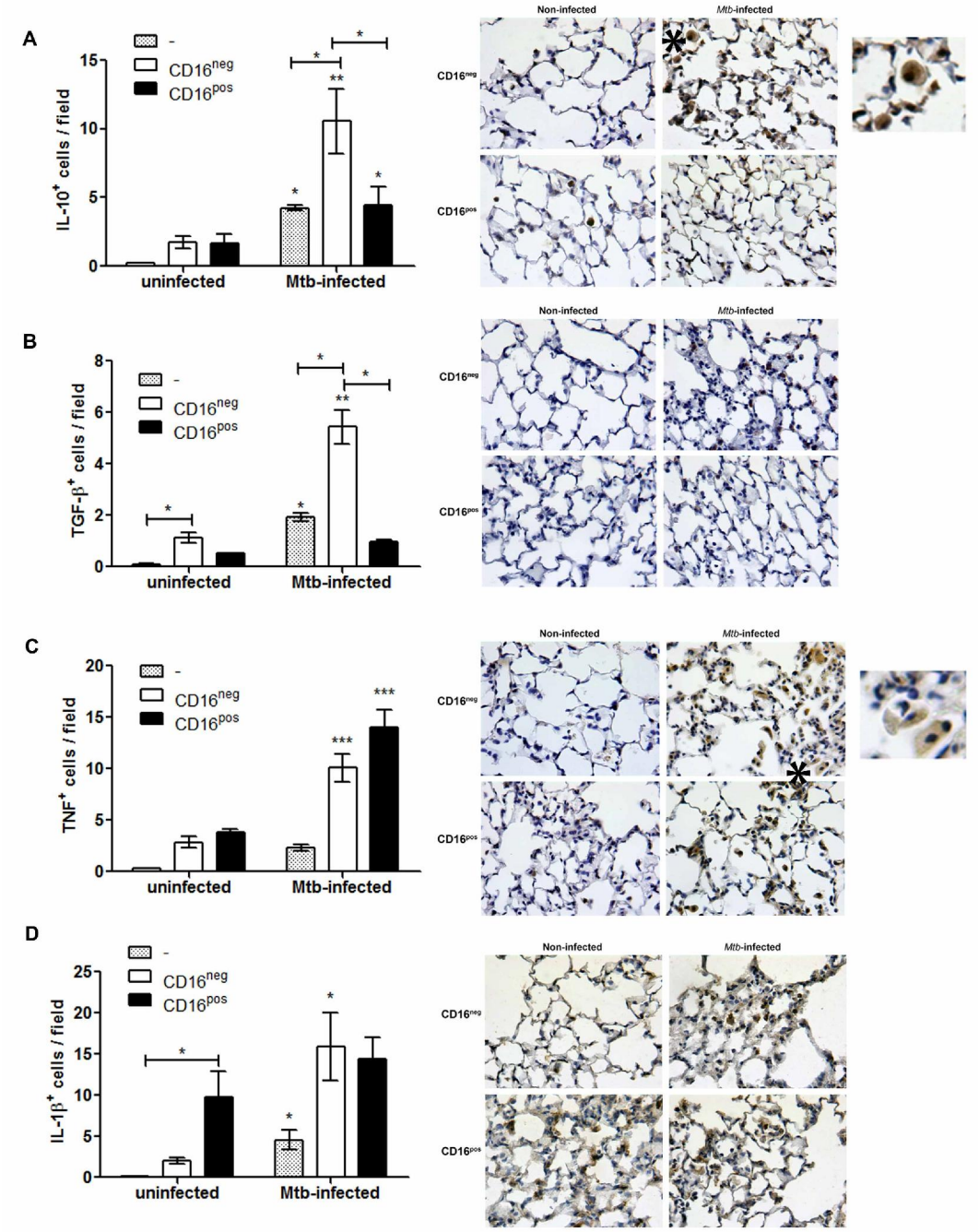

Figure 3. Modulation of local cytokines production by CD16^{neg} and CD16^{pos} Mo. The production of IL-10 (A), TGF-β (B), TNF (C), and IL-1β (D) in lungs from non-transferred (-), CD16^{neg} or CD16^{pos}-transferred *Mtb*-infected or uninfected SCID/Beige mice determined by IHC. The percentages of positive cells per field are the mean ± SEM of eight independent experiments, considering fifteen random fields. Statistical analysis: **P* < 0.05, ***P* < 0.01, ****P* < 0.001, *Mtb*-infected vs uninfected, or comparisons are indicated by lines. Representative micrographs of cytokines detection by IHC comparing infected and non-infected mice, transferred with CD16^{neg} or CD16^{pos} Mo are shown (400x magnification, haematoxylin counterstain). Macrophages showing an activated phenotype are visualized (asterisks) in *Mtb* infected mice transferred with CD16^{neg} Mo.

Figure 4

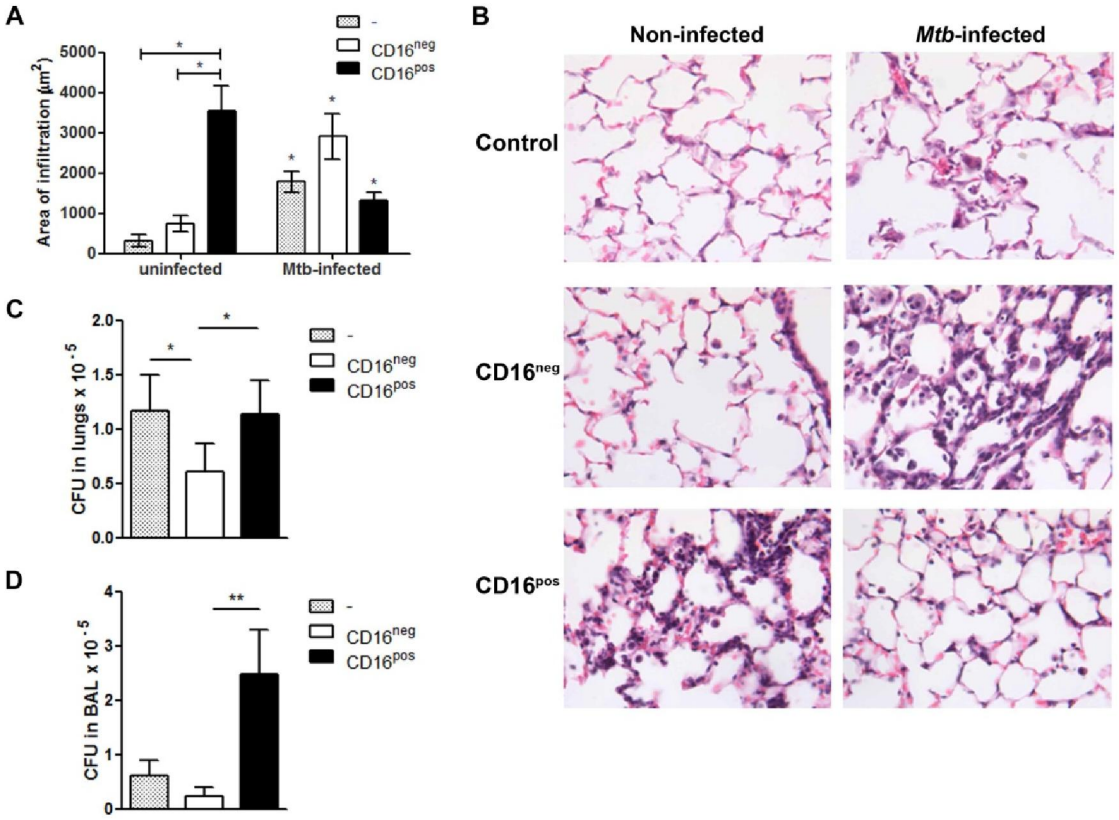

Figure 4. Impact on pulmonary cell recruitment and mycobacterial loads after CD16^{neg} and CD16^{pos} Mo transference. (A) Morphometric analysis of the inflammatory infiltrate into lungs from non-transferred (-), CD16^{neg} or CD16^{pos}-transferred *Mtb*-infected or uninfected SCID/Beige mice. Results are the mean ± SEM of five independent experiments, considering fifteen random fields. (B) Representative micrographs showing the histopathological findings in the lungs from non-transferred (control), CD16^{neg} or CD16^{pos}-transferred *Mtb*-infected or uninfected SCID/Beige mice (400x magnification, haematoxylin–eosin staining). (C and D) Bacterial burdens were determined in the lungs (C) and BAL (D) in non-transferred (-), CD16^{neg} or CD16^{pos}-transferred *Mtb*-infected SCID/Beige mice at 24 hours post-infection. Results are the mean ± SEM of eight independent experiments. Statistical analysis: **P*< 0.05, ***P*<0.01, vs control.

Summary statement

We demonstrated divergent roles of human monocyte subsets throughout the course of the *M. tuberculosis* infection. While $CD16^{neg}$ monocytes may contribute to the anti-mycobacterial immune response, $CD16^{pos}$ monocytes might promote microbial resilience.

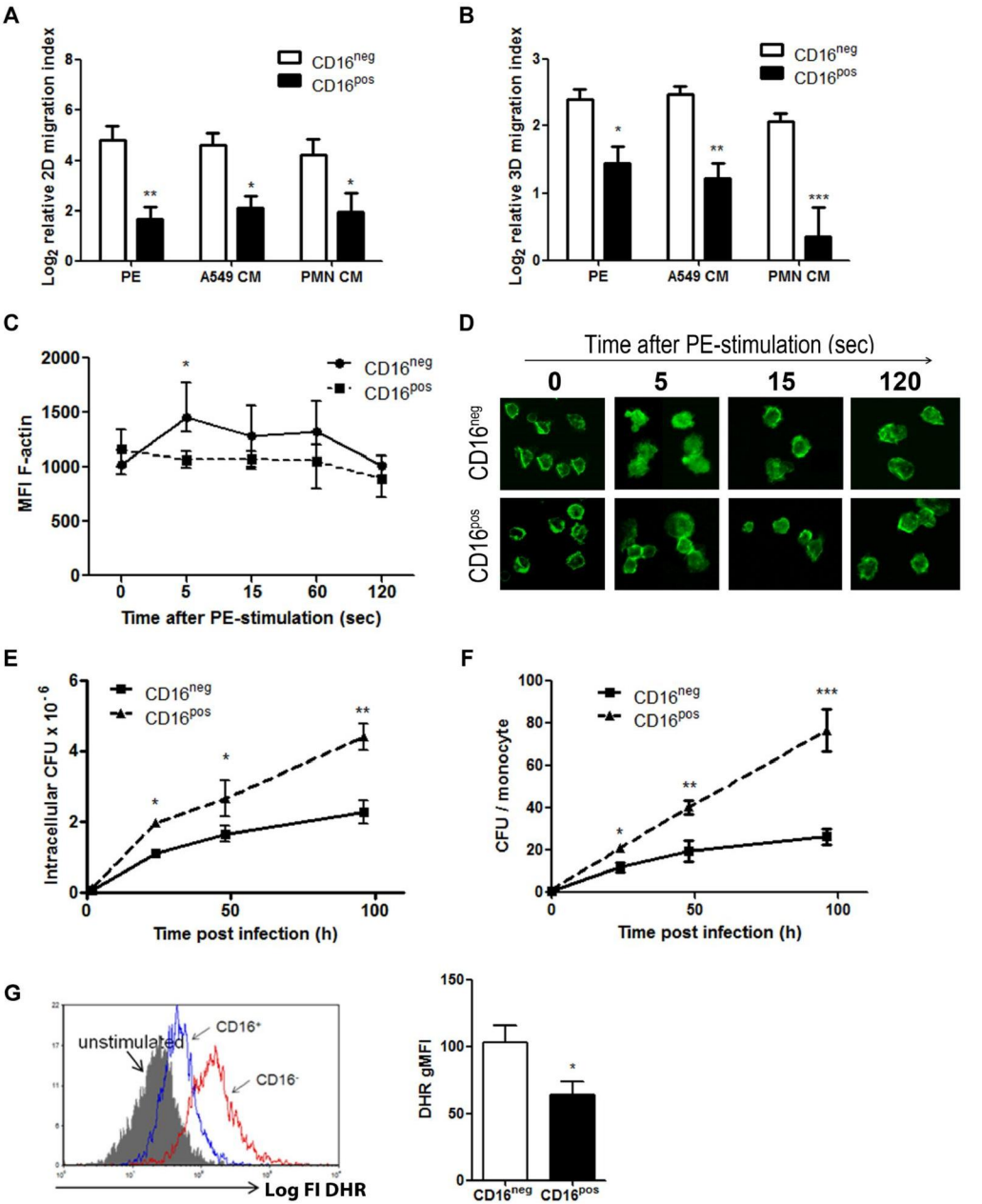
A
Log2 relative 2D migration index
CD16neg
CD16pos
PE
A549 CM
PMN CM
B
Log2 relative 3D migration index
C
MFI F-actin
Time after PE-stimulation (sec)
D
Time after PE-stimulation (sec)
0
5
15
120
E
Intracellular CFU x 10-6
Time post infection (h)
F
CFU / monocyte
G
unstimulated
CD16+
CD16-
Log FI DHR
DHR gMFI

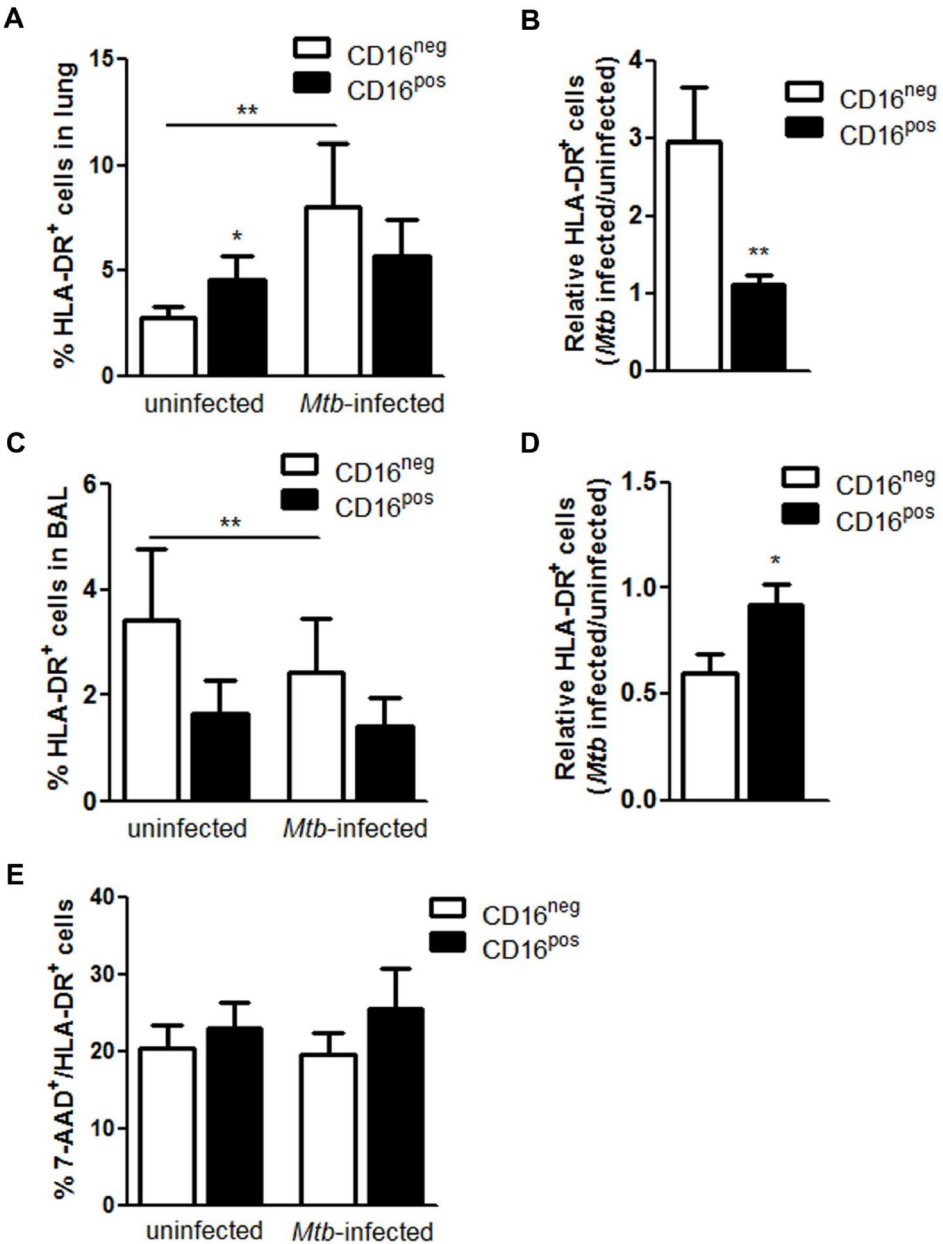
A
% HLA-DR+ cells in lung
CD16neg
CD16pos
uninfected
Mtb-infected
B
Relative HLA-DR+ cells (Mtb infected/uninfected)
C
% HLA-DR+ cells in BAL
D
Relative HLA-DR+ cells (Mtb infected/uninfected)
E
% 7-AAD+/HLA-DR+ cells

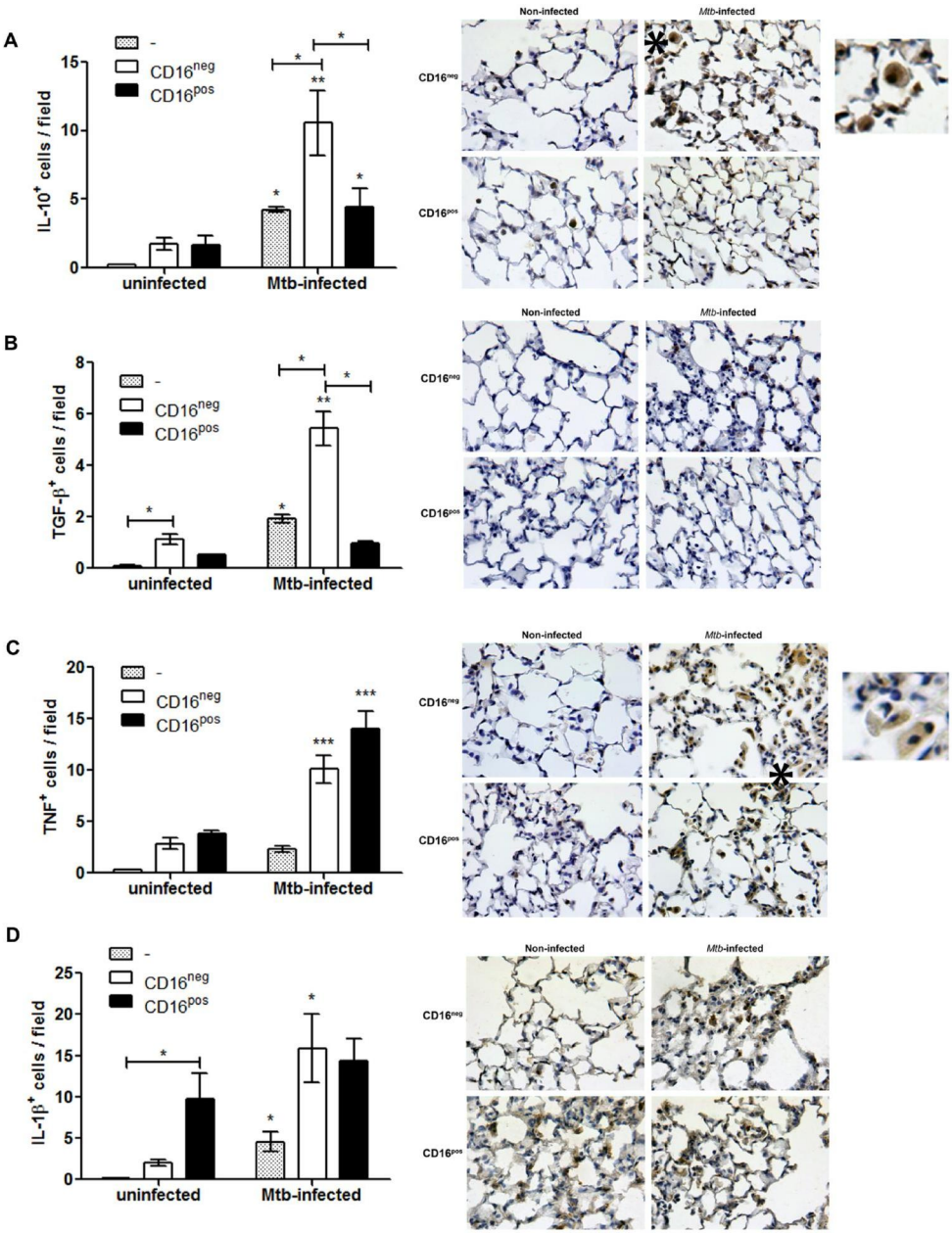
A
IL-10+ cells / field
-
CD16neg
CD16pos
uninfected
Mtb-infected
Non-infected
Mtb-infected
CD16neg
CD16pos
B
TGF-β+ cells / field
C
TNF+ cells / field
D
IL-1β+ cells / field

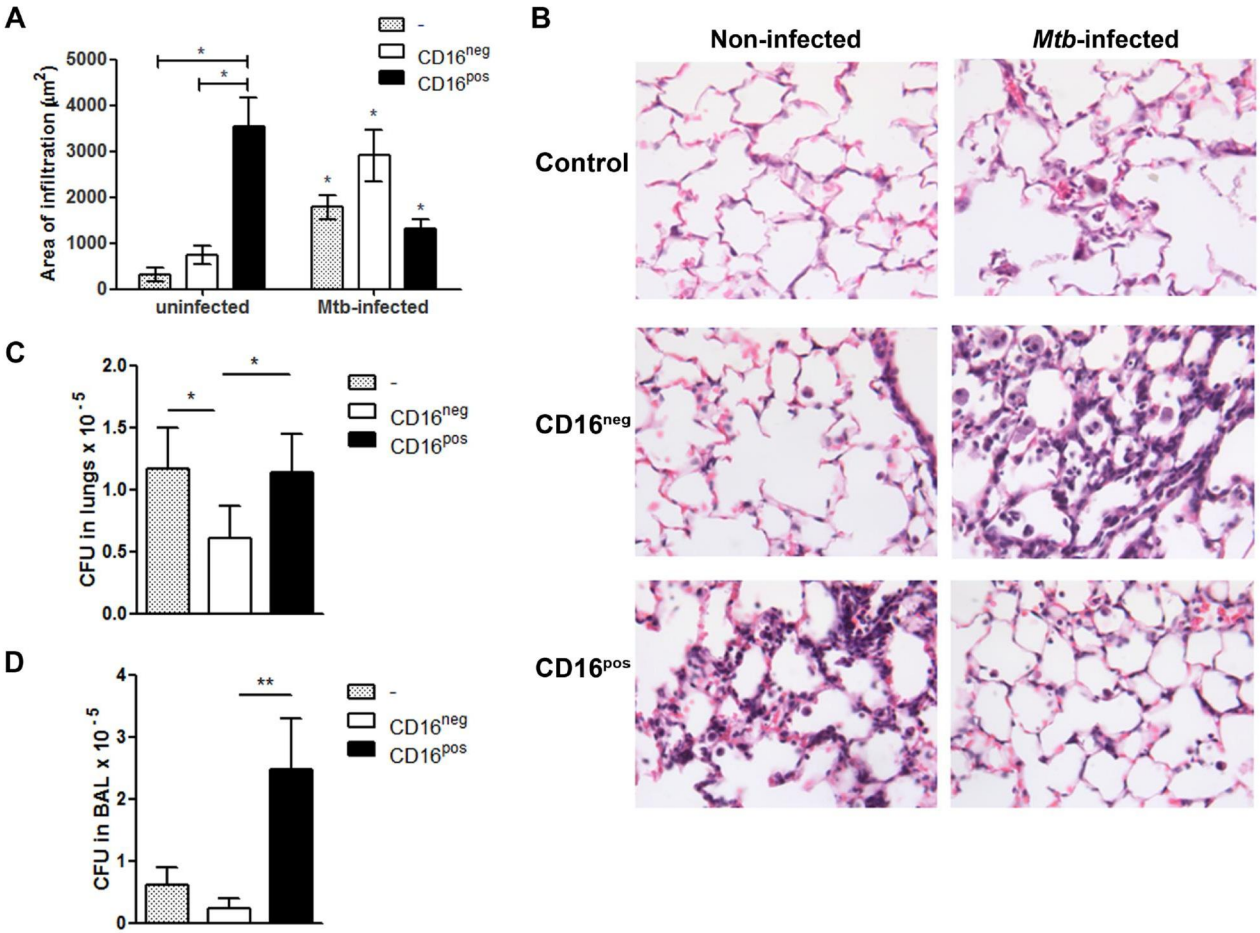
A
Area of infiltration (µm²)
5000
4000
3000
2000
1000
0
uninfected
Mtb-infected
-
CD16neg
CD16pos
B
Non-infected
Mtb-infected
Control
CD16neg
CD16pos
C
CFU in lungs x 10⁻⁵
2.0
1.5
1.0
0.5
0.0
D
CFU in BAL x 10⁻⁵
4
3
2
1
0